Th/K and Th/U ratios from spectral gamma-ray surveys improve the mapped definition of subsurface structures

Ruffell, A., McKinley, J., Lloyd, C., & Graham, C. (2006). Th/K and Th/U ratios from spectral gamma-ray surveys improve the mapped definition of subsurface structures. Journal of Environmental and Engineering Geophysics, 11 (1)(1), 53-61. DOI: 10.2113/JEEG11.1.53

Published in:
Journal of Environmental and Engineering Geophysics

Th/K and Th/U Ratios from Spectral Gamma-Ray Surveys Improve the Mapped Definition of Subsurface Structures

A. Ruffell*, J.M. McKinley, C.D. Lloyd and C. Graham
School of Geography, Queen's University, Belfast, N. Ireland

*Corresponding author. E-mail: a.ruffell@qub.ac.uk

ABSTRACT

Spectral gamma-ray data can be obtained by non-destructive, automated, rapid and inexpensive survey methods. Previous studies utilise only total count, or total count as well as K, U and Th data. This work examines the use of Th/K and Th/U ratios to define the subsurface extent of partially-buried features at the centimeter to meter scale. On-site results are presented from two case studies as two-dimensional cross-sections. Changes in Th/K and Th/U ratios coincide with the known location of buried structures to within 10 cm horizontal resolution. Gradual changes in total count, K, U and Th measurements give a lower horizontal accuracy of 30 cm to 1 m. Grids of data were manipulated in ArcGIS™ using a thin plate spline function to maximise information use and provide 'easy to interpret' maps of the survey areas. Unlike total count or individual element maps, Th/K and Th/U ratio maps can be compared to the known location of subsurface structures, vindicating the use of ratio cross-sections and maps in archaeological, geotechnical and forensic applications. It is concluded that the capacity to observe sub-surface features is enhanced through the use of Th/K and Th/U ratios.

Introduction

Gamma-ray and spectral gamma-ray surveying relies on spatial variations in the distribution of Earth materials that contain radiation-emitting isotopes. Gamma-ray surveys have traditionally been used *either* over large areas (generally airborne, kilometer-scale) for mineral prospecting (Darnley and Ford, 1987) and radiation hazard assessment (Jones *et al*., 2002) or down boreholes (at centimeter-scale) for rock petrophysics (Kearey *et al*., 2002). Applications of the gamma-ray technique to smaller-scale (centimeters to meters) spatial archaeological and geotechnical surveys have been limited to crude spatial measurements of total count, K (potassium)-, U (uranium)- and Th (thorium)-based radiation (Ruffell and Wilson, 1998; Moussa, 2001). Consequently, while measurement of K, U and Th inter-elemental ratios have been routine in large-scale surveying (Shives *et al*., 1997) and in borehole logging (Davies and Elliot, 1996), mapping the spatial variation in spectral gamma-ray ratios at centimeter- to meter-scale has never been attempted.

This work uses two case studies to describe the rationale for measuring and mapping Th/K and Th/U ratios. We use a combination of field-based total count, K, U, Th, Th/K and Th/U ratio cross-sections in order to determine whether a survey should continue. These single-transect cross-sections also allow some limited, onsite comparison to observed features. When an area is mapped, we have then used thin plate splines to produce greyscale maps of variation: these show how Th/K and Th/K have the capacity to define subsurface features better than single element or total count maps.

Spectral Gamma-Ray Emission

At the Earth's surface, gamma-rays may be encountered that have emanated from natural or anthropogenic sources. These may be detected with a Geiger-Muller Tube and scintillation type detector. Natural sources of gamma-rays include radioactive isotopes in rocks, soils and water or from outer space. Anthropogenic sources include processed isotopes of, for example, uranium, cesium, californium and others for nuclear power generation, medical uses and weapons manufacture. The isotopic source of gamma-rays may be discovered by use of a spectral gamma-ray detector, a device that measures characteristic gamma-ray wavelengths. In this study, the naturally-occurring gamma-ray radiation of ^{40}K, ^{238}U and ^{232}Th are utilised.

The usefulness of spectral gamma-ray data originates with mineralogical variation controlling the sites in which K, U and Th may reside. K is common in many sediments that bear K-feldspar, micas, clays or salts. Uranium (U) and thorium (Th) have a number of host minerals in sedimentary rocks including clays (including illite and kaolinite), micas (including biotite), feldspars, heavy minerals (including monazite, thorite, uraninite), phosphates (calcium flourapatite)

and organic matter. In fine-grained sediments most U and Th is sited in clays, organic matter (where present) and heavy minerals. Heavy minerals such as zircons, uraninites and thorites have high Th or U, creating a potential problem when interpreting the gamma-ray emission of sediments with heavy mineral contents (Hurst, 1990). U is considered soluble in neutral (pH 7) aqueous fluids and more prone to mobilisation than Th during leaching and clay mineral diagenesis. This is especially true for weathering, which commonly occurs under oxidising conditions, where U and K are easily mobilised but Th is not. The presence of organic acids complicates this simple pattern, as Th will be mobilised. Under oxidising weathering conditions, away from the presence of humic acids, Th/U ratios from the same sample or location may show similarities to Th/K ratios (Rosholt, 1992; Osmond and Ivanovich, 1992).

Gamma-Ray Mapping in Subsurface Analysis

In geological studies, gamma-ray transects or mapping have been utilised for many years in the search for mineralised zones (Ford, 1993), either for nuclear energy or as a proxy for radon hazard (Kearey *et al*., 2002). Such studies employ either total count scintillation or spectral detectors in aircraft or vehicles because the K, U or Th bearing rocks and minerals being sought emit high levels of gamma-rays. The application of gamma-ray detectors to surficial sediments has followed two courses of research: airborne, hazard detection or mineralisation studies (Tyler, 1999; El Nabi, 1995; Chiozzi *et al*., 1998) and surface, archaeological and geotechnical studies (Ruffell and Wilson, 1998; Gautam *et al*., 2000; Moussa, 2001; Ayres and Theilen, 2001; Jones *et al*., 2002). All of these applications have been made possible through the development of highly-sensitive, weatherproof, automated, spectral gamma-ray detectors.

Nonetheless, there are still only two published papers concerning the use of spectral gamma-ray surveying in the subsurface mapping of buildings or archaeological remains (Ruffell and Wilson, 1998; Moussa, 2001). Neither of these works utilise elemental ratios of the different isotopes detected. Kilometer-scale mapping and small-scale (centimeter-scale) stratigraphic (vertical) logging using Th/K and Th/U ratios have both proven useful, cost-free additions to these datasets, providing the impetus for the current work. The airborne and surface surveys cited above have utilised total count detection, together with spectral information from specific natural and anthropogenic isotopes. In the geological (stratigraphic) use of spectral gamma-ray information, In sediments, Th contents were found to be low and scattered compared to K and Th (Davies and Elliot, 1996): Th ratios have aided further data analysis by providing a less variable gamma-ray source, independent of K or U. The non-destructive, portable and rapid method of deriving spectral gamma-ray data makes it worthwhile generating ratio transects or maps. As we show in this study, these can prove informative on their own and even more useful when interpreted in conjunction with the conventional (total-count, K, U and Th) spectral gamma-ray data.

Methods

Data Acquisition

Total count and spectral gamma-ray measurement using a spectral gamma-ray detection device is a frequently-used and standard geophysical technique (Kearey *et al*., 2002). A Scintrex GIS-5 portable gamma-ray detector was used for its small size, flexibility of data collection modes and rugged, waterproof makeup. The device uses a $3.7 \times 3.7 \times 5.0$ cm^3 thallium-activated sodium iodide (NaI(Tl)) crystal detector. The detector converts an absorbed gamma ray into a light pulse with an energy proportional to the energy of the incident ray. The light pulse is transformed into an electrical pulse by a photo-multiplier tube (PMT). The different energies are then sorted, or stripped from one another by amplitude. The detection is made by combination of the scintillation crystal and PMT.

The resolution of different energies is dependant on the makeup of the scintillator. Light to electrical energy pulses measured by devices such as the Scintrex GIS-5 are sorted according to amplitude by switching the device to record energy within these four windows. First, total count (TC) measures all gamma-ray energy above 0.05 MeV. This measurement number is always higher than the combined K, U and Th as other radionuclides contribute to the gamma-rays detected at this energy level. Second, K, U and Th is measured at all energies above 1.38 MeV. Third, U and Th are measured at 1.66 MeV or above, effectively removing the K^{40}-sourced energy. Fourth, and last, Th is estimated by measuring all energy at 2.38 MeV, which is significantly higher than the U window.

In natural environments, where there is a mixture of K, U and Th emitters, we can only guess at the hosts of these different gamma-rays. It is possible for gamma-ray energies not to be separated within the resolution of the detector. For U and Th this is not a problem as their decay will emit several gamma-rays within the time measurement, allowing measurement of activity. However, K may generate gamma-rays at 1,460.8 Ke V and Th at 1,459.2 Ke V, which are practically coincident. In the majority of sample locations in this study (and in general, throughout our experience), K emissions average 10 times that of Th, allowing easy correction based on the various spectral peaks of Th. If Th emission approaches that of K, then it becomes impossible to differentiate K and Th. This was not a problem in this study, but as beach sands do

contain thoriferous heavy mineral lags, similar studies may run into problems.

What can be done is comparison of individual K, U and Th outputs, where similarities may be a function of common host, or of gamma-rays from one isotope entering the window of another. Measurements made using a Scintrex GIS-5 machine were calibrated to a Th standard (Scintrex GIS-5 User Manual) and deployed at a 25 cm sample distance on a grid over the survey area: the device has a theoretical 'cone' of subsurface detection, 20 to 30 cm in diameter at the surface. Thus, a potential overlap with neighboring sample sites occurs, depending on levels of gamma-ray emission. Measurements taken at greater spacing than 60 cm may not detect significant changes or sources of gamma-rays: measurements taken at less than 20 cm spacing may detect gamma-rays from the same source, for which a mathematical adjustment can be made.

The square root of each measured number provides an estimate of statistical uncertainty. The published and tested methodologies of Slatt *et al*. (1992) and Hadley *et al*. (2000) were followed, wherein five readings were taken at each site, the lowest and highest were discarded and the three remaining averaged. This widely-published method has proven very reliable in removing gamma-ray emission that is unrelated to the average, long-term signal of the survey area. The repeatability and accuracy of the Scintrex GIS-5 was checked using an Exploranium GR256 Spectrometer on 20% of the survey area, as this device takes longer to measure each location. The operational limitations and detection limits of both these machines are described by Slatt *et al*. (1992) and Davies and Elliot (1996), respectively.

Data Manipulation in the Field

We devised a method of field testing whether ratio measurements were likely to improve the horizontal location of features in the subsurface. This method comprised plotting simple cross-sections of total count (TC), K, U, Th and ratios of test sections, adjacent to where we could visually identify changes in the near-surface. This may comprise a survey line a few centimeters from where a pipe or wall became submerged by soil or sediment. The steepness of the sections at likely subsurface boundaries gave an indication of the probable horizontal accuracy of mapped images. Following initial sectional surveys, the survey grid layout could be adjusted to cross major structures at 90°. In the case study locations, the general trend of the partially-buried structures was known; but in the future, completely-buried structures will benefit from the above reconnaissance, transect survey, followed by a complete grid.

Post-acquisition Data Manipulation—
Thin Plate Splines (TPS)

Following the survey, data were reformatted in x,y,z format and grey-scale intensity maps generated using the thin plate spline functionality of ArcGIS. Thin plate splines provide a means of making predictions at locations where there are no measurements—in this case the gaps in the data are replaced by predicted values and a map that is smoother in appearance than the original data grid is produced. Thin plate smoothing splines are fitted to the $z(\mathbf{u}_\alpha)$, $\alpha = 1, 2, \ldots n$, data points closest to an unsampled location at which a prediction is to be made. The spline must fit the data points sufficiently closely while being as smooth as possible (Hutchinson and Gessler, 1994; Wackernagel, 2003). The objective is to estimate a smooth function g by minimizing:

$$\sum_{\alpha=1}^{n} (z(\mathbf{u}_\alpha) - g(\mathbf{u}_\alpha))^2 + \rho J_m(g) \tag{1}$$

where $J_m(g)$ is a measure of the roughness of the spline function g (defined in terms of mth degree derivatives of g) while $\rho > 0$ is a smoothing parameter. The function $g(\mathbf{u})$ is the sum of two terms:

$$g(\mathbf{u}) = \sum_{l=1}^{M} a_l f_l(\mathbf{u}) + \sum_{\alpha=1}^{n} \lambda_\alpha R(\mathbf{u}, \mathbf{u}_\alpha) \tag{2}$$

where $f_l(\mathbf{u})$ are a set of M monomials and $R(\mathbf{u}, \mathbf{u}_\alpha)$ is a basis function. For TPS the basis function, $R(\mathbf{u}, \mathbf{u}_\alpha)$, is $d_i^2 \log d_i$, where $d_i^2 = (x - x_i)^2 + (y - y_i)^2$. The coefficients a_l and λ_α are the solution of:

$$\begin{pmatrix} \mathbf{R} + \lambda\mathbf{I} & \mathbf{F} \\ \mathbf{F}^{\mathrm{T}} & \mathbf{0} \end{pmatrix} \begin{pmatrix} \lambda \\ \mathbf{a} \end{pmatrix} = \begin{pmatrix} \mathbf{z} \\ \mathbf{0} \end{pmatrix} \tag{3}$$

The application of the TPS function can be problematic in areas. Predicted values from TPS are not limited within maximum and minimum values of known points (unlike with other interpolation methods such as inverse distance weighting). Large gradients can be produced in data-poor areas producing overshoots (Chang, 2002). A second problem is that the second-order derivatives diverge in the data points. TPS with tension (TPST) provides one solution to these problems. The tension can be changed so that the surface may resemble a stiff plate or an elastic membrane (Mitáš and Mitášová, 1999). For TPST (Franke, 1985) the basis function for two dimensions is:

$$-\frac{1}{2\pi\phi^2}\left(\ln\left(\frac{d\phi}{2}\right) + C_E + K_0(d\phi)\right) \tag{4}$$

where ϕ is the tension parameter, $C_E = 0.577215 \ldots$ (the Euler constant) and $K_0(d\phi)$ is an approximation of the modified zeroth-order Bessel function (Mitáš and Mitášová, 1988). Chang (2002, page 288) provides a worked example of TPST.

In this paper, the functionality of ArcGIS Geostatistical Analyst (Johnston *et al*., 2001) is used to make

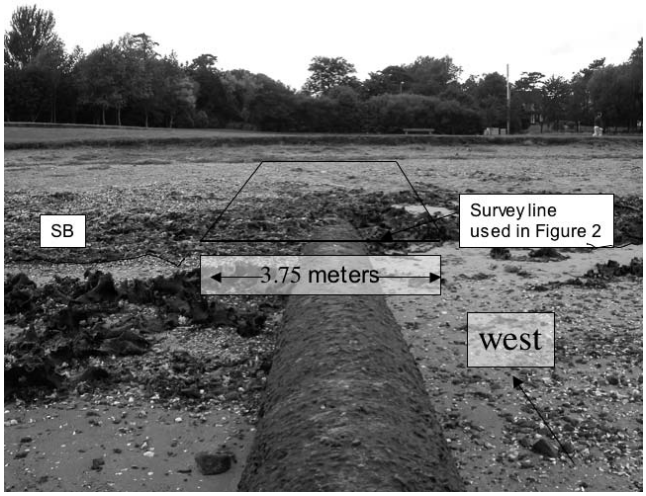

Figure 1. Ratio mapping Site 1. Sewage outfall, Loughshore Park, Jordanstown, Co. Antrim. (IGR 366834 5°53′W 54°41′N). SB = storm beach (line at which the survey area is covered). The location of the cross section shown in Fig. 2 (coincident with eastern side of survey) is shown.

spatial predictions using TPST. In other words, predictions were made at a finer grid than that on which data were available. Using the software, the tension of the spline can be selected using a cross-validation procedure.

Case Studies

Study I: Partially-buried Buried Sewage Outfall Pipe

Description and results. To test a simple survey area, the location of a known buried structure was surveyed. The target comprised a 45-year old land drainage pipe (Fig. 1) that crosses (sequentially) a major roadway, a sandy soil playing field (subject to the application of K-fertiliser), a beach (dominated by quartz and calcite sand) and emerges at the high-tide zone of an estuary (Belfast Lough, N. Ireland). The pipe emerges at a level of the beach that is 35 cm below the highest level of the adjacent playing field. Assuming that the pipe has a gentle seaward dip (to enable runoff), the greatest depth at which the pipe is buried in the survey grid is probably 30 cm.

The pipe is approximately 110 cm across and has walls of 12 cm thickness. These are constructed of concrete (calcium carbonate–sand mix), with unknown sand origin. The pipe has an associated outer fill (variable width between 5 cm and 25 cm) of basalt aggregate in asphalt. Survey limits included 50 cm of the exposed pipe, coincident with the high-tide mark. The survey was conducted 2 days after a period of rainfall, resulting in flushing of saltwater from the sediment and reducing the highly unlikely complication of seawater or evaporated seawater K influencing the readings.

On-site, south to north cross-sections of total count, spectral, and ratio measurements (Fig. 2) indicated that the

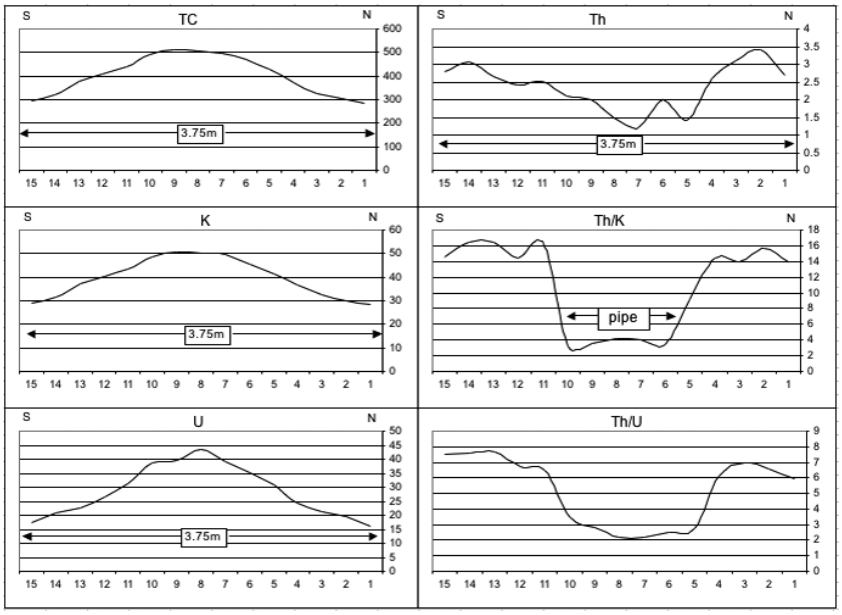

Figure 2. Spectral gamma-ray measurement cross-sections taken from the first line of the survey at Site 1 (location on Fig. 1). This section was constructed in the field in order to confirm that Th/K and Th/U ratios might prove more precise than conventional data. x-axis = position on survey line. y-axis = counts per 30 seconds (average of three readings). Note how the edges of the sewage pipe are defined accurately on the Th/K cross section. No corrections have been applied to this data (see "Methods—data acquisition").

results showed potential and the survey was worth continuing. In particular, elevated total counts, K and U measurements defined the location of the pipe, but Th/K and to a lesser extent, Th/U showed a sharp fall at the edges of the known location of the pipe, indicating that serial sections, or a mapped output of gridded Th ratio data would show a well-defined line coincident with the buried portion of the pipe. The mapped grid across the pipe (Fig. 3) confirms the on-site indication that Th/K and Th/U ratios enable an accurate prediction of the subsurface extent of the structure.

Gamma-ray radiation is dominated by K and U, demonstrated by the nearly-identical total count and K map and very similar total count and U map. The Th/K map shows excellent definition of the edges of the sewage pipe, including what appears to be a 20–40 cm long dislocation on the southern (left) side of the pipe at 150 cm from the eastern (shoreline) edge of the survey. The Th/U map shows better definition than the total count of spectral maps, but is not as precise in showing the edges of the pipe as the Th/K map. Nonetheless, the Th/U map shows consistent NW-SE features crossing the pipe.

Interpretation. K and U dominate the total count gamma-ray radiation across the sewage pipe: their similar distribution suggests a common host or control on location. That K contents remain unchanged along the length of the pipe suggests that a seawater contribution is either minimal or extends well inland: the latter is unlikely given the continual flushing of the pipe. Thus, the K is likely derived from soil clay minerals and K-feldspars in the basalt aggregate concrete of the pipe and surrounding foundations. U contents may likewise be accounted for by soil clay minerals and organic matter. The more scattered, low-abundance distribution of Th is typical of the clay mineral hosts in soils (Ruffell and Wilson, 1998; Moussa, 2001; Jones *et al*., 2002). This may be explained through low quantities of the likely host clay minerals and isolated thoriferous heavy minerals.

The improved visible detail of the mapped data is partly a function of decisions made when using thin plate splines. The field-based cross-sections indicate that the improved mapped image of Th ratios over conventional total count, K, U or Th data is dependant on the plotting of ratios. Th/K ratios fall dramatically at the edge of the pipe as K contents rise by a factor of 3 compared to only 1.5 in Th. This creates an "edge effect" with the pipe but is so dramatic it obscures some detail. Th/U demonstrates that some subtle variation can be detected within the pipe signal, although whether this is above, within, or below the pipe is not known: given the low penetrating power of gamma-rays, this signal most likely relates to features at 0–30 cm depth, or the top of the pipe. The coincidence of Th/K dislocation with one such NW-SE oriented feature suggests that these features are associated with a structure in the pipe itself.

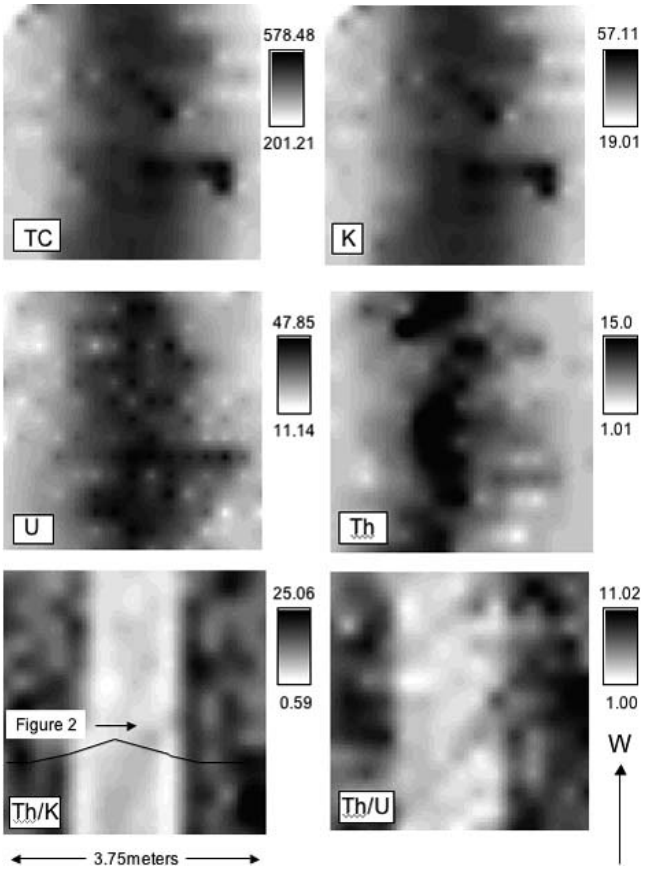

Figure 3. Gamma-ray total count (TC), spectral gamma-ray (K, U and Th) and derived ratio maps of Site 1. Plots generated in ArcGIS using thin plate spline with tension. The extent of the sewage pipe (including a potential change of size) is clear on the plot of Th/K. SB = limit of storm beach: the pipe is covered from this line westwards. The section shown in Fig. 2 is indicated.

These may be U-rich sediment layers or organic matter-filled fractures. The consistent orientation of this feature precludes it from being an artifact from the TPS output. The tar in the asphalt may contain U, but would be unlikely to host significant K. It would be coincidental for the asphalt aggregate to contain a K source independent of the tar, such as K-feldspars.

Case Study II: Partially-buried House Foundation

Description and results. The second test site comprises a partially-buried house foundation with complex geometry, limited foundation exposed at surface and a complicating adjacent stream (Fig. 4). The site was a house from 1890 to 1970, when it was levelled in order to create further flat ground for the positioning of static caravans: the site (now marked by a concrete post) is the present (2004) limit of a holiday caravan park. This survey area is located at the southern end of Ballywalter Beach, County Down

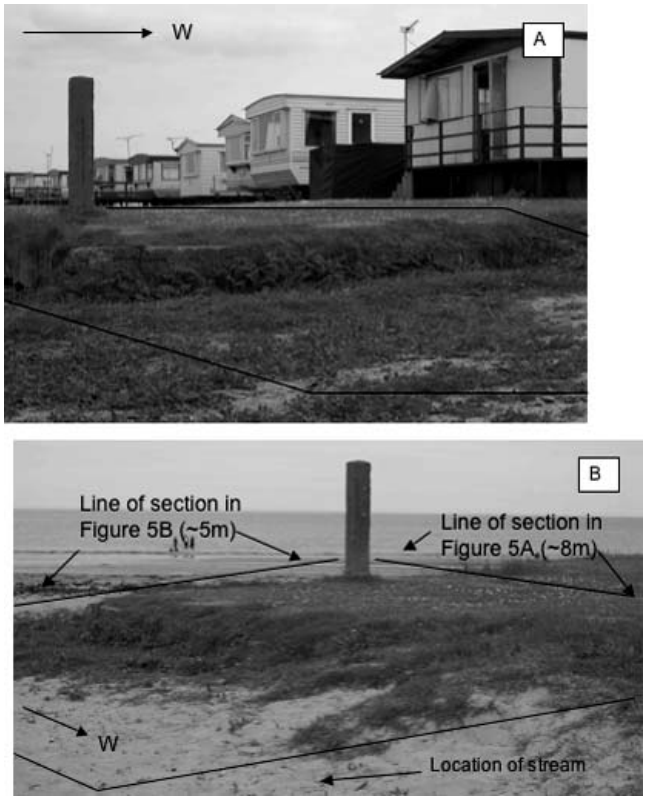

Figure 4. Ratio mapping Site 2. Ballywalter Beach (southern end, IGR 635676; 5°28′W 54°31′7″N). A. View to the south-east, showing overview of site. B. View to the east, with location of cross-sections.

(N. Ireland), on the margins of the Irish Sea. The exposed foundations (comprising a 3 m × 2 m corner) are constructed of double-thickness red-brick and weathered rubble infill with a combined width of 50 cm. The bricks are set in a loose aggregate of brick, greywacke and concrete rubble. The foundations are presumed to continue into the subsurface where they are covered by a sandy soil (a few centimeters to 30 cm thick). A stream runs parallel to the western edge of the foundation at a distance of 5 meters. The stream bed is filled with peat and rotting seaweed but was freshwater on the seven times the site was visited over one year. Spring tides reach to within 4 meters of the edge of the site.

On-site, east–west and north–south cross-sections of total count, spectral, and ratio measurements indicated that the results showed potential and the survey was again worth continuing (Fig. 5).

Elevated total counts, K, U and Th in the southern part of the survey area matched the location of the exposed corner of the foundation. Th/K showed a sharp fall at the edges of the known location of the foundation, continuing under the sand and soil. These sections indicated that serial sections, or a mapped output of gridded data would generate a map that was partially coincident with the rest of the foundations. The mapped grid (Fig. 6) showed that although total count, K and U variations may be compared to the foundations, these data were confused by elevated counts adjacent to the banks of the stream. The mapped data confirm the on-site indication from cross-sections of the increased resolution of Th/K (and to a lesser extent, Th/U) ratios. Gamma-ray radiation is dominated by U and to a lesser amount, K. The Th/K ratio map (Fig. 6) defined a 20 cm-wide, south to north oriented feature from 40 cm north of the exposed corner of the foundation, extending toward the stream.

Interpretation. U and K dominate the natural gamma-ray radiation source of this site. U shows a close visual match to the total count, although the narrow extent of low Th/U ratios shows that elevated U is of more significance on the southern and western, inner parts of the foundations than on the former outside of the house. K is derived from clay minerals in the aggregate or bricks and K-feldspars in the crushed greywacke concrete foundations. The distribution of U is coincident with the foundations and results from clays, greywacke micas and organic matter in otherwise U-poor quartz sands. Th distributions are very scattered, as found in the above sewage pipe case study and in other studies (Ruffell and Wilson, 1998; Moussa, 2001). This is again explained through the likely host clay and isolated thoriferous heavy minerals. Th/K ratios fall dramatically at the edge of the foundations as K contents are elevated. The stream sediments are interpreted to influence total count, K, U, Th and Th/U as a west–east oriented line of elevated counts extends along the north edge of the foundations: alluvial heavy minerals may be present in these sediments. Th/K ratio mapping minimises this influence and instead defines the south–north ratio "low": this may well be a trench or pipe extending from the former house to the stream. From this survey we cannot determine whether this north-south feature is above, below, or at the same level as the foundations. Figure 6 shows a visual indication of the feature being below the foundation, which excavation or a depth survey such as ground-penetrating radar would assess. Th/K shows the clear "edge effect," coincident with the foundations and similar to Case Study I (sewage pipe). Again, the inner, high U area of the former house is brought out in the Th/U, suggesting a subtle difference in the Th/K and Th/U data.

Conclusions

On the kilometer to hundreds of meters scale that two previous studies of spectral gamma-ray survey have been conducted (Ruffell and Wilson, 1998; Moussa, 2001), total counts, K, U and Th data have been adequate in defining the limits of foundations, pipes and mining activity. This is confirmed in the current study. On the decameter scale of

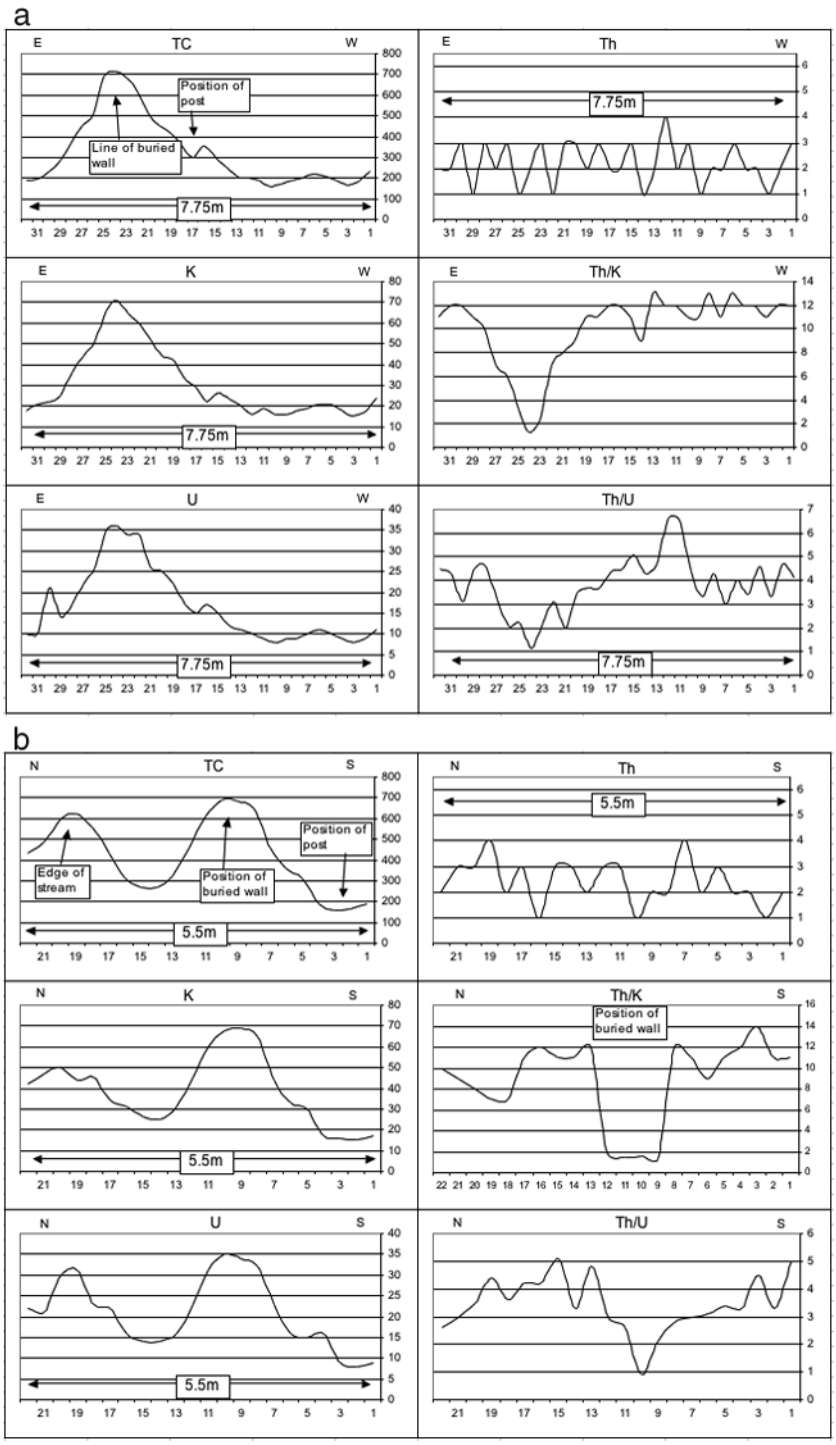

Figure 5. a) Spectral gamma-ray cross-sections taken from the first line of the survey (east to west) at Site 2 (location on Figs. 4 and 6). The section was constructed in the field in order to assess survey orientation and ratio accuracy. X-axis = position on survey line. Y-axis = counts per 30 seconds (average of three readings). b) Spectral gamma-ray cross-sections taken from the second line of the survey (north–south) at Site 2 (location of Figs. 4 and 6). Note how the position of the buried wall is shown accurately on the Th/K cross-section. X-axis = position on survey line. Y-axis = counts per 30 seconds (average of three readings).

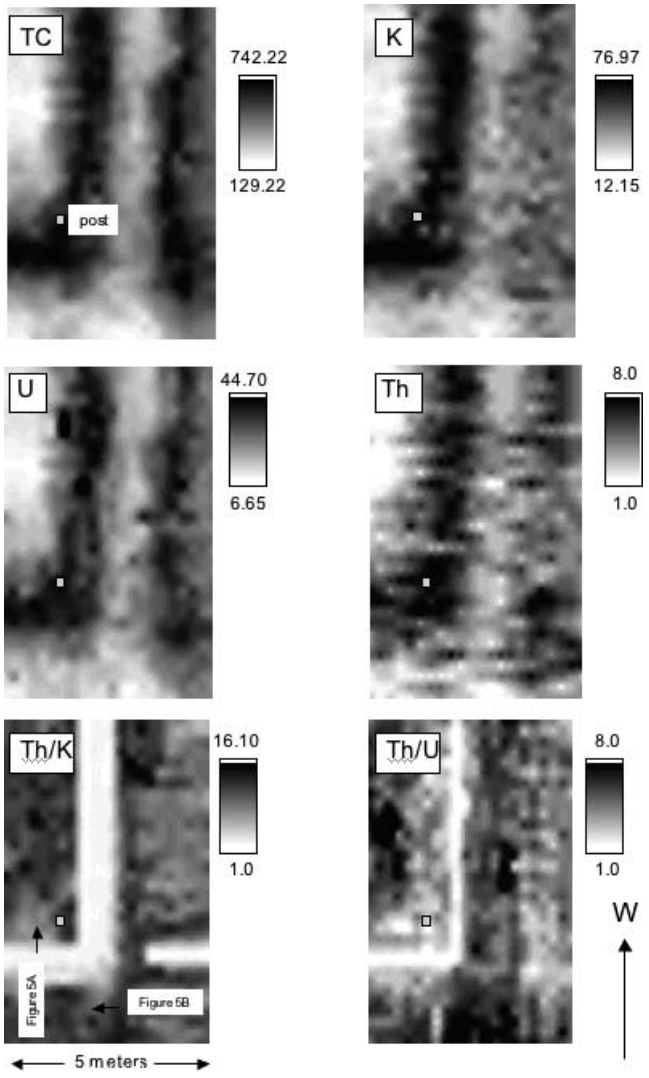

Figure 6. Gamma-ray total count (TC), spectral gamma-ray (K, U and Th) and derived ratio maps of Site 2. The concrete post on Fig. 4 is shown in order to aid location. Plots generated in ArcGIS using thin plate spline with tension. The extent of the foundation is clear on the plot of Th/K. The section shown in Fig. 5 is indicated.

this work, variations in conventional (non-ratio) spectral gamma-ray data do coincide with buried pipes and foundations. In both cases, crude on-site, Th/K ratio sections and thin plate spline derived maps best define the location and extent of subsurface structures, with the edges of buried structures being well-imaged compared to total count or single-element distributions. We suggest that Th/K shows well-defined but less consistent along-strike measurements when compared to Th/U, which showed a less precise definition of the edge of the structures, but that were considered geometrically realistic. We strongly suggest that all the described techniques (total count, K, U, Th, their ratios and TPS mapped outputs) should be used in conjunction and never alone, and emphasise that important information may be held in each dataset. The increased interpretative power of spectral gamma-ray ratio maps, produced using thin plate spline with tension, has been demonstrated for these two shoreline locations. Future work should take this technique to other locations, possibly in clay-rich ground and other marginal marine locations, to examine whether ratio maps can image what conventional spectral gamma-ray surveys and possibly other geophysical devices cannot. Some of this work may not even require new surveys as pre-existing gamma-ray data at any resolution may be formatted into ratios and manipulated in GIS software, other contouring software packages, or serial sections from spreadsheets.

Acknowledgments

AR thanks David Jones (British Geological Survey), Mohamed Moussa (Suez Canal University) and Andrew Tyler (University of Stirling) for their help in discussions. This work was presented at an Environmental and Industrial Geophysics Group meeting of the Geological Society (London) on improvements in pavement imaging, organised by Chris Leech. The helpful comments of referees and editors Kulessa and Nyquist improved the work greatly.

References

Ayres, A., and Theilen, F., 2001, Natural gamma-ray activity compared to geotechnical and environmental characteristics of near surface sediments: Journal of Applied Geophysics, **48**, 1–10.

Chang, K., 2002, Introduction to geographic information systems: McGraw-Hill, Boston.

Chiozzi, P., Pasquale, V., and Verdoye, M., 1998, Ground radiometric survey of U, Th and K on the Lipari Island, Italy: Journal of Applied Geophysics, **38**, 209–217.

Darnley, A.G., and Ford, K.L., 1987, Regional airborne gamma-ray surveys: A review. In Exploration '87. Proceedings Geophysical Methods, Advancements in the State of the Art.

Davies, S.J., and Elliott, T., 1996, Spectral gamma ray characterization of high resolution sequence stratigraphy: Examples from Upper Carboniferous fluvio-deltaic systems, County Clare, Ireland: *in* High resolution sequence stratigraphy: Innovations and applications, Howell, J.A., and Aitken, J.F. (eds.), Geological Society Special Publication, **104**, 25–35.

El Nabi, S.H.A., 1995, Statistical evaluation of airborne gamma-ray spectroscopic data from the Magal Gebriel area, south Eastern Desert: Journal of Applied Geophysics, **42**, 105–112.

Ford, K.L., 1993, Radioelement mapping of parts of the Musquodoboit Batholith and Liscomb complex, Meguma zone Nova Scotia: *in* Mineral deposit studies in Nova Scotia, Volume 2, Sangster, A.L. (ed.), Geological Survey of Canada, Paper 91-9, 71–111.

Franke, R., 1985, Thin plate splines with tension: Computer Aided Geometric Design, **2**, 87–95.

Gautam, P., Raj Pant, S., and Ando, H., 2000, Mapping subsurface karst structure with gamma ray and electrical resistivity profiles: A case study from Pokhara: Journal of Applied Geophysics, **45**, 97–110.

Hadley, M.J., Ruffell, A.H., and Leslie, A.G.L., 2000, Gamma-ray spectroscopy in structural correlations: An example from the Neoproterozoic succession of Donegal (NW Ireland): Geological Magazine, **137**, 137–152.

Hurst, A., 1990, Natural gamma-ray spectrometry in hydrocarbon-bearing sandstones from the Norwegian continental shelf: *in* Geological applications of wireline logs, Hurst, A., Lovell, M., and Morton, A. (eds.), Geology Society London Special Publication, **48**, 211–222.

Hutchinson, M.F., and Gessler, P.E., 1994, Splines—More than just a smooth interpolator: Geoderma, **62**, 45–67.

Johnston, K., Ver Hoef, J.M., Krivoruchko, K., and Lucas, N., 2001, Using ArcGIS™ geostatistical analyst: ESRI, Redlands, California.

Jones, D., Limburg, J., and Dienst, R.O.E.Z., 2002, Use of gamma-ray spectrometry for Archaeological site investigations: Abstract "Recent Work in Archaeological Geophysics", Environmental and Industrial Geophysics Group Meeting, Burlington House, London, 17th December, 2002.

Kearey, P., Brooks, M., and Hill, I., 2002, An introduction to geophysical exploration: Blackwell Scientific Publishers, 280 pages.

Mitáš, L., and Mitášová, H.H., 1988, General variational approach to the interpolation problem: Computers and Mathematics with Applications, **16**, 983–992.

Mitáš, L., and Mitášová, H.H., 1999, Spatial interpolation: *in* Geographical information systems. Volume I: Principles and technical issues, 2nd ed., Longley, P.A., Goodchild, M.F., Maguire, J.D., and Rhind, D.W. (eds.), John Wiley and Sons, New York, 481–492.

Moussa, M., 2001, Gamma-ray spectrometry: A new tool for exploring archaeological sites: A case study from East Sinai, Egypt: Journal of Applied Geophysics, **48**, 137–142.

Osmond, J.K., and Ivanovich, M., 1992, Uranium-series mobilisation and surface hydrology: *in* Uranium-series disequilibrium: Applications to earth, marine and environmental sciences, Ivanovich, M., and Harmon, R.S. (eds.), Clarendon Press, Oxford, 259–289.

Rosholt, J.N., 1992, Mobilisation and weathering: *in* Uranium-series disequilibrium: Applications to earth, marine and environmental sciences, Ivanovich, M., and Harmon, R.S. (eds.), Clarendon Press, Oxford, 167–178.

Ruffell, A., and Wilson, J., 1998, Shallow ground investigation using radiometrics and spectral gamma-ray data: Archaeological Prospection, **5**, 203–215.

Shives, R.B.K., Charbonneau, B.W., and Ford, K.L., 1997, The detection of potassic alteration by gamma-ray spectrometry—Recognition of alteration related to mineralization: *in* Gubins, A.G. (ed.), Proceedings of Exploration '97: Fourth Decennial International Conference on Mineral Exploration, 741–752.

Slatt, R.M., Jordan, D.W., D'Agostino, A., and Gillespie, R.H., 1992, Outcrop gamma-ray logging to improve understanding of subsurface well log correlations: *in* Geological applications of wireline logs II, Hurst, A., Griffiths, C.M., and Worthington, P.F. (eds.), Geological Society Special Publication, **65,** 3–19.

Tyler, A.N., 1999, Monitoring Anthropogenic Radioactivity in Salt Marsh Environments through in situ gamma ray spectrometry: Journal of Environmental Radioactivity, **45**, 235–252.

Wackernagel, H., 2003, Multivariate geostatistics: An introduction with applications, 3rd ed.: Springer, Berlin.